A New Approach for Pulsating Torque Minimization of BLDC Motor

Young-Jin Lee*, Man Hyung Lee
School of Mechanical Engineering, Pusan National University, Pusan 609-735, Korea
Sung-Jun Park
Department of Electrical Engineering, Dong-Myong College, Pusan 608-740, Korea
Han-Woong Park
Department of Electrical Engineering, Korea Naval Academy, Kyungnam 645-031, Korea

Torque ripple control of brushless DC motor has long been the main issue of the servo drive systems in which the speed fluctuation, vibration and acoustic noise need to be minimized. The vast majority of the methods for suppressing the torque ripple require the Fourier series analysis and either the iterative or least mean square minimization. In this paper, a novel approach based on the d-q-0 reference frame that achieves ripple-free torque control with maximum efficiency is presented. The proposed method optimizes the reference phase current waveforms including even the case of 3-phase unbalanced condition, and the motor winding currents are controlled to track the optimized current waveforms by the delta modulation technique. As a result, the proposed approach provides a simple and yet effectine means for obtaining the optimal motor excitation currents. The validity and applicability of the proposed control scheme are verified through simulations and experimental investigations.

Key Words : Brushless DC Motor, Torque Ripple, Maximum Efficiency, Optimal Current

1. Introduction

Brushless permanent magnet motors (BLPMs), in which the most popular back EMF waveform is trapezoidal, are increasingly being used in high performance applications due to their simple control. In many of these applications, the production of ripple-free torque in the motor is of primary concern. There are three main sources of torque production in BLPMs; cogging torque, reluctance torque, and mutual torque. The cogging torque is created by the stator slots interacting with the rotor magnetic field and is independent of the stator current excitation. The reluctance torque is caused by the variation in the phase inductance with respect to the position. The mutual torque is created by a mutual coupling between the stator winding current and rotor magnetic field. Therefore, if the waveforms of the phase back EMF and phase current are perfectly matched to produce the required load torque and eliminate the first two torque components, the torque ripple can be minimized.

A great deal of study has been devoted to identifying the sources illucidating their characteristics, and devising the means for minimizing the torque ripple. In particular, the interaction between the back EMF and the current excitation has been described and analyzed by a number of authors (Le-Huy, etd., 1986; Hung and Ding, 1992; Hanselman, 1994). LeHuy, Perret and Feuillit (1986) determing that the torque ripple can be minimized by appropriately selecting the current harmonics to eliminate both the excitation

* Corresponding Author,
E-mail : yjlee4@hyowon.pusan.ac.kr
TEL : +82-51-583-5812 ; **FAX** : +82-51-516-5891
School of Mechanical Engineering, Pusan National University, San 30, Jangjeon-dong, Keumjung-ku, Pusan 609-735, Korea. (Manuscript **Recieved** May 30, 2000; **Revised** April 10, 2001)

and cogging torque ripple components. Hung and Ding(1992) used the complex exponential decomposition to find a closed form solution for the current harmonics that eliminate the torque ripple and maximize the efficiency simultaneously. Hanselman(1994) extended these prior works to the case of a finite supply voltage and resulting finite di/dt capability. All these works have made several limiting assumptions that all three phases have an identical back EMF waveforms offset by $2/3\pi$[rad] electrical angle with respect to one another and that the back EMF and motor excitation current exhibit half-wave symmetry, among others. Among them, Hung and Ding(1992) and Hanselman(1994) and be easily extended to the more general case where the above assumptions need not be made. In practice, due to several reasons such as manufacturing imperfections, deterioration of permanent magnets or unbalanced stator windings, etc, making these assumptions can lead to an undesirable error. In addition, if the motor has four or more poles, the phase back EMF waveform from one cycle to the next may be different because of the unbalanced magnetization of the magnets and/or manufacturing errors.

This paper deals with the new torque control scheme based on the d-q-0 reference frame for BLPMS at low speeds with maximum efficiency, including the cases when the 3 phase stator windings are unbalanced and the phase back EMF waveform from one cycle to the next is different. The phase back EMF waveforms in the natural a-b-c reference frame are transformed to the d-q-0 reference frame. Only the quadrature component that contributes to the production of the mutual torque, is accounted for by equating the electrical power absorbed by the motor to the mechanical power that includes the reluctance and cogging torque components. Consequently, the optimum phase current waveforms can be obtained by inversely transforming the d-q-0 variables to a-b-c variables. The motor winding currents are forced to track the optimal current waveforms by the delta modulation technique. Simulation and experimental results are presented to illustrate the validity and appliability of the proposed control scheme.

2. Proposed Approach

Figure 1 shows the configuration of the BLPM under test. To analyze and develop the proposed torque control scheme, the following simple assumptions are made in this paper.

1) The three phase stator windings are Y-connected.

2) The mutual torque produced by the motor is linearly proportional to the phase current.

3) The mutual inductance between phases is negligible.

4) DC source voltage is infinite and is capable of delivering infinite di/dt.

Given the above assumptions, the equivalent circuit of BLPM with the PWM inverter is modeled as in Fig. 2, where N', N are the neutral points of the inverter and motor, respectively.

Figure 3 shows the measured phase back EMF waveforms of the BLPM under test. As shown in the figure, three back EMFs are slightly different in magnitude and shape from one another, and the corresponding phase currents should also be

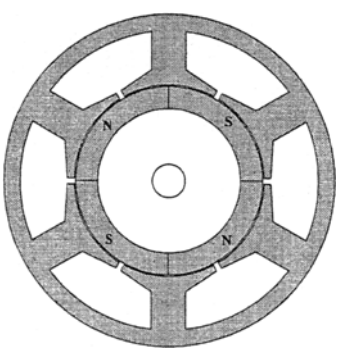

Fig. 1 The BLDC motor configuration

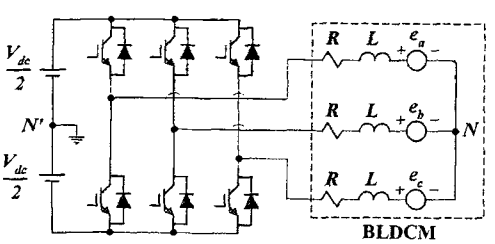

Fig. 2 PWM inverter and equivalent circuit of BLPM

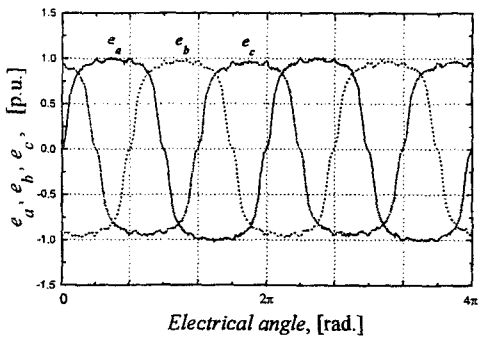

Fig. 3 The measured phase back EMF waveforms

different. In addition, if the motor has four or more poles, the back EMF waveforms from one cycle to the next may be different because of the dimensional and magnetization unbalance of the magnets and/or manufacturing errors. Therefore, the back EMF waveform of one cycle of the mechanical angle, which is equal to two cycles of the electrical angle for four pole motor, should be incorporated to control the instantaneous torque.

Therefore, for maximum efficiency a new torque ripple minimization approach based on the d-q-0 reference frame is presented in this paper. In general, the stator windings of the BLPM are concentrated and the air-gap flux density by the rotor magnet can be considered to be a square wave. Consequently, it can be argued that since the stator to rotor mutual inductance does not vary sinusoidally, the synchronously rotating d-q reference frame analysis is no longer valid except only when the harmonic components of field distribution and inductance variation are considered. However, d-q-0 reference frame approach adopted in this paper will be used only to obtain the optimum current waveform for the ripple-free torque based on the minimum input power, and not for modeling and simulation of the motor itself. It can be considered as an another harmonic current injection method that is yet different from the previous works involving the Fourier analysis. Hence, the proposed method can be a proper choice. In addition, the zero sequence variables must be taken into account because of the unbalances among the phase windings and the discrepancy between the cycles of the phase back EMF. The proposed approach has the following features.

1) An alternative simple method is presented.

2) Phase commutation needs not be considered.

3) Assumptions such as the shape, magnitude and half-wave symmetry of each phase back EMF need not be made.

The optimum current waveforms for each phase by the proposed method can be obtained as follows. Firstly, the phase back EMF waveforms in the natural a-b-c reference frame are transformed to the d-q-0 reference frame.

$$\begin{bmatrix} e_d \\ e_q \\ e_0 \end{bmatrix} = C \cdot \begin{bmatrix} e_a \\ e_b \\ e_c \end{bmatrix} \tag{1}$$

$$C = \frac{2}{3}\begin{bmatrix} \sin(\theta_e-\theta_0) & \sin\left(\theta_e-\theta_0-\frac{2\pi}{3}\right) & \sin\left(\theta_e-\theta_0+\frac{2\pi}{3}\right) \\ \cos(\theta_e-\theta_0) & \cos\left(\theta_e-\theta_0-\frac{2\pi}{3}\right) & \cos\left(\theta_e-\theta_0+\frac{2\pi}{3}\right) \\ \frac{1}{2} & \frac{1}{2} & \frac{1}{2} \end{bmatrix}$$

where $\theta_e=\omega_e t$, ω_e is the electrical angular frequency and θ_0 is the angular displacement between the stator and rotor flux linkage and C is the transformation matrix of 3 phase to the synchronously rotating d-q-0 reference frame. In the d-q-0 reference frame, the mutual torque is derived by equating the electrical power absorbed by the motor to the mechanical power produced as follows.

$$\tau_L \frac{\omega_e}{P} = \frac{3}{2}(e_d i_d + e_q i_q + e_0 i_0) \tag{2}$$

where τ_L is a ripple-free torque required by the load, and P is the number of pole pairs and ω_e/P is the motor mechanical speed. Considering that the magnetic field of the BLPM is provided by the permanent magnet in the rotor and also that the sum of the phase current must be zero at any instant, the current components i_d as well as i_0 associated with the field and zero sequence flux generation must be zero. Therefore Eq. (3) can be rewritten as

$$\tau_L \frac{\omega_e}{P} = \frac{3}{2} e_q i_q \tag{3}$$

From the above equation, i_q component can be obtained as follows.

$$i_q=\frac{2}{3}\tau_L\frac{\omega_e}{P}\frac{1}{e_q} \tag{4}$$

Each optimum phase current waveform can be derived by transforming the d-q-0 variables to the a-b-c variables inversely.

$$\begin{bmatrix} i_a \\ i_b \\ i_c \end{bmatrix}=C^{-1}\cdot\begin{bmatrix} i_d \\ i_q \\ i_0 \end{bmatrix} \tag{5}$$

It should be emphasized that in order to minimize losses and maximize the torque per ampere, each phase current must be excited in phase with the corresponding phase back EMF, i. e., $\theta_0=0$ must be substituted in C matrix in Eq. (5). This will be discussed in the next section.

3. Numerical Results

The phase back EMF waveform is measured by the constant speed test for a 400 W, 4 pole, Y -connected, 100 V BLPM. Each back EMF waveform is normalized by the peak value of the phase a having the highest value among the phases. The optimization procedure corresponding to Eqs. (1) ~ (5) is performed to generate the current profiles which produce the desired torque with minimum pulsation. For simplicity, the cogging torque is not incorporated in this case. There are numerous current profiles that produce torque without any pulsation below the base speed. This is illustrated in Fig. 4(a) for phase c when the current leads back EMF by the angles of $\pi/12$, $\pi/6$, $\pi/4$ (dotted lines) and lags by the same angles (thin solid lines). Figure 4(b) also shows the calculated torque profiles corresponding to each current profile. The current profile denoted by the thick solid line is in phase with the back EMF and is optimum, because it exhibits the highest value of torque per ampere and does not produce negative torque at any instant as shown in Fig. 4(b).

Figure 5 shows the simulation results of the proposed approach using the measured back EMF waveforms without considering the cogging torque. Figure 5(a) shows the back EMF components of the d-q-0 reference frame obtained from Eq. (1). The torque current i_q is obtained from e_q

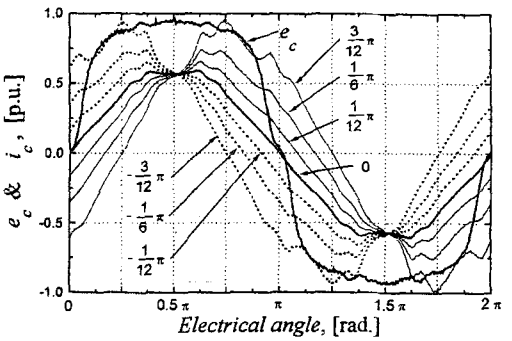

(a) The phase current profiles for produing ripple free torque

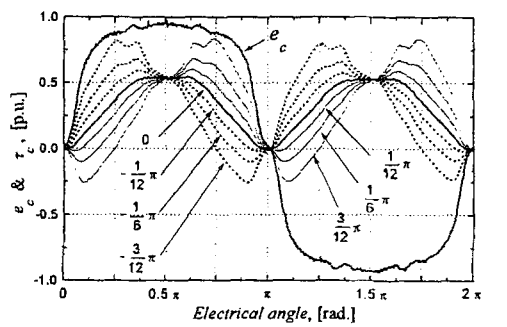

(b) The corresponding phase torpue profiles

Fig. 4 The phase current and corresponding torque profiles that produce ripple free torque for phase c back EMF

by Eq. (4) and i_d and i_0 must be zero as shown in Fig. 5(b). The instantaneously optimized phase currents that are obtained from Eq. (5) are shown in Fig. 5(c). The phase currents are slightly different in shape and magnitude and do not exhibit half-wave symmetry. But it is guaranteed that the sum of the currents is zero at any instant and the commutation problem between the phases can be eliminated. The corresponding phase and total torque profiles are presented in Fig. 5(d). In this case, the phase torque profiles are also different from each other as expected from the current and back EMF waveforms, but the total torque exhibits no pulsation as shown in the figure. These results show that the proposed control scheme for the torque ripple elimination can be quite effective.

Similary, the optimum phase current considering the cogging torque can be obtained by simply adding the cogging torque component to the

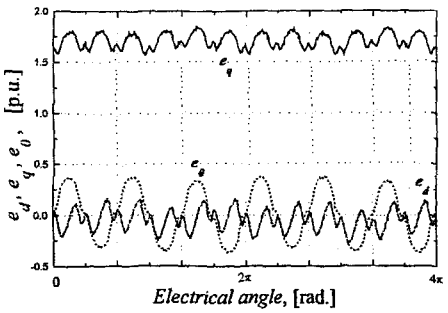

(a) e_d, e_q, e_0 waveforms

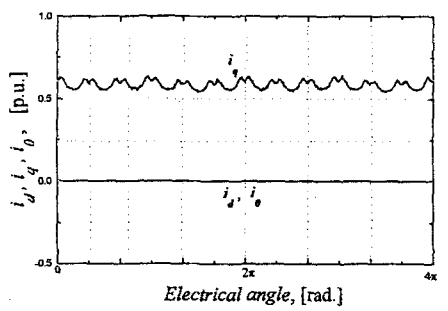

(b) Desired i_d, i_q, i_0 waveforms

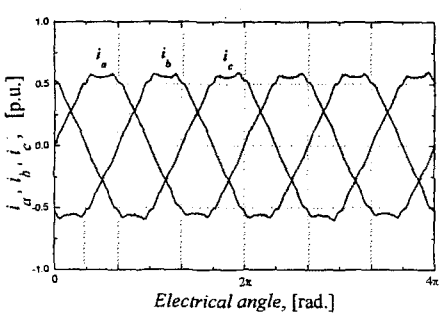

(c) Desired i_a, i_b, i_c waveforms

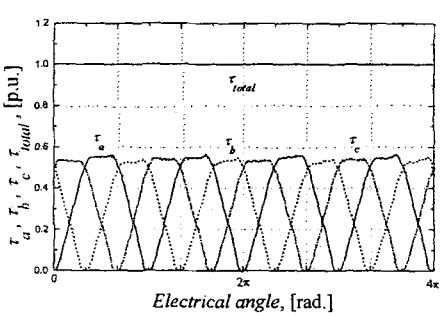

(d) Total and phase torque waveforms

Fig. 5 Simulation results of the proposed control scheme of BLPM without considering the cogging torque

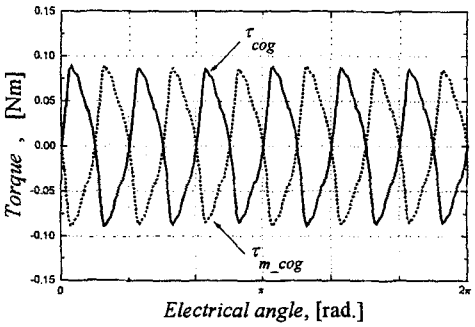

(a) Measure cogging torque τ_{cog} and mutual torque τ_{m-cog} for compensating the cogging torque

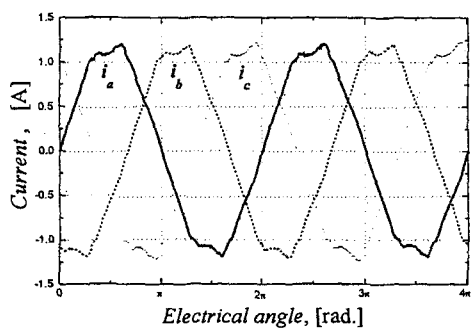

(b) Optimized phase current waveforms for ripple-free torque including cogging torque

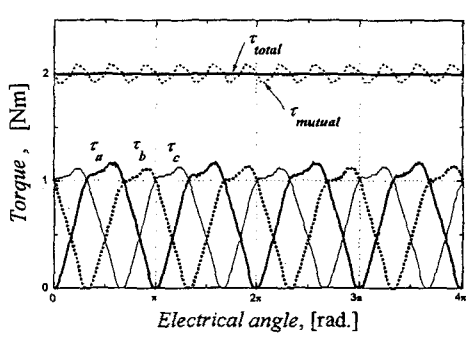

(c) Waveforms of the optimized torque per phase τ_a, τ_b, τ_c, and total mutual torque τ_{mutual} and resultant developed torque τ_{atotal} at the motor shaft

Fig. 6 Simulation results of the proposed control scheme of BLPM with considering the cogging torque

required load torque component in Eq. (4). The measured cogging torque component τ_{cog} around the airgap is shown in Fig. 6(a) (solid line). To eliminate the ripple torque caused by the cogging torque, an additional mutual torque τ_{m-cog} are required as shown in the same figure (dotted

line). To produce the load torque and compensate for the cogging torque, the optimized phase current waveforms can be obtained by performing the same procedure as shown in Fig. 6(b). As a result, the resultant torque τ_{total} is produced as shown in Fig. 6(c), which also shows the waveforms of the phase torque τ_a, τ_b, τ_c and the resultant mutual torque τ_{mutual}.

4. Experimental Results

To ensure the validity of the proposed method, it is required to measure the actual torque. Ideally, the torque can be calculated by differentiating the mechanical speed, but the direct differentiation enlarges the noise component. Therefore, the torque observer as shown in Fig. 7 is used to monitor the real torque.

$$\dot{\mathbf{x}}=\mathbf{A}\hat{\mathbf{x}}+\mathbf{B}\mathbf{u}+\mathbf{L}(\mathbf{y}-\mathbf{C}\hat{\mathbf{x}}),\ \mathbf{y}=\mathbf{C}\hat{\mathbf{x}}$$

where

$$\mathbf{A}=\begin{bmatrix} B/J & 1/J \\ 0 & 0 \end{bmatrix},\ \mathbf{B}=\begin{bmatrix} 0 \\ 0 \end{bmatrix},\ \mathbf{C}=[1\ 0]$$

$$\hat{\mathbf{x}}=\begin{bmatrix} \hat{\omega}_m \\ \hat{\tau}_e \end{bmatrix},\ u=0,\ y=\hat{\omega}_m,\ \mathbf{L}=\begin{bmatrix} l_1 \\ l_2 \end{bmatrix}$$

L : observer gain matrix,
B : viscous damping constant,
J : moment of inertia,
$\hat{\omega}_m$: estimated speed,
$\hat{\tau}_e$: estimated torque

The mechanical torque equation is given as follows

$$J_m\frac{d\omega}{dt}+B_m\omega=\tau_e+\tau_L$$

where ω : mechanical angular speed of rotor
J_m : Moment of inertia
B_m : Damping coefficient

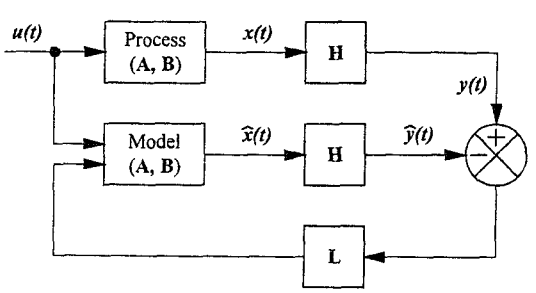

Fig. 7 Block diagram of the observer

τ_e : Electromagnetic torque
τ_L : Load torque

Comparing the characteristic equation of the state observer model with the roots of the observer error, the parameters of the matrix L can be obtained.

Because a fast and accurate measurement of the mechanical speed is critical for estimating the instantaneous torque, a high precision encoder of 40,000 pulses per revolution is attached to the motor shaft. M/T method is used for the measurement of the speed. The sampling time interval is about 200 μs and measurement error for the worst case is less than 0.3 r/min. This error corresponds to 0.06 Nm or 0.025 p. u. of torque error. The estimated speed and torque are only for monitoring, and the real position and speed feedback for the controller are given by the encoder of 500 pulses per revolution which represents a rather low precision.

The proposed method with the torque observer is implemented using the high performance digital signal processor (DSP) TMS320C40. The sampling time of the torque controller is 100 μs, and the switching frequency is 5 kHz.

A speed control scheme of the proposed approach is shown in Fig. 8. The back EMF data corresponding to the rotor position are measured and set up in the look-up table. The optimized reference current waveforms are obtained from the look-up table using the position and speed information from the shaft encoder PE1. The motor currents are compared and forced to track the reference currents within the predetermined bandwidth by the delta modulation technique. The peripheral devices with high speed switching are selected to utilize the DSP effectively, the

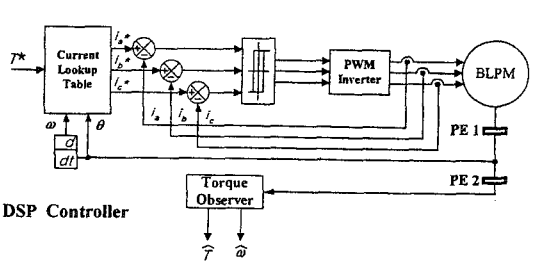

Fig. 8 Block diagram of the speed control scheme of the proposed approach

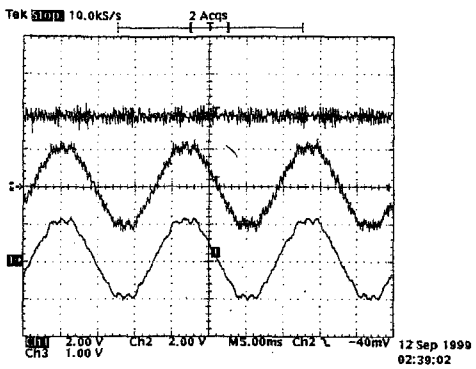

current : 3 [A/div.]

torque : 0.5 [Nm/div.]

(a) When the cogging torque is considered

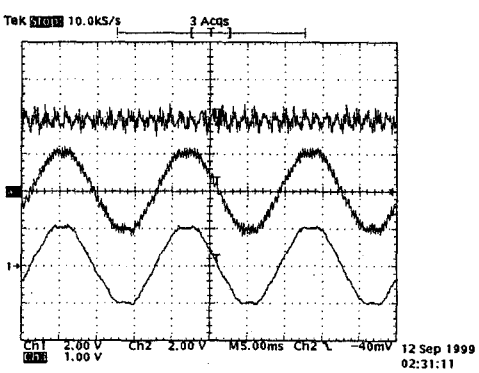

current : 3 [A/div.]

torque : 0.5 [Nm/div.]

(b) When the cogging torque is not considered

Fig. 9 The experimental results of the proposed control scheme of BLPM when the motor speed is 1,800 rpm, the load torque is 1 Nm

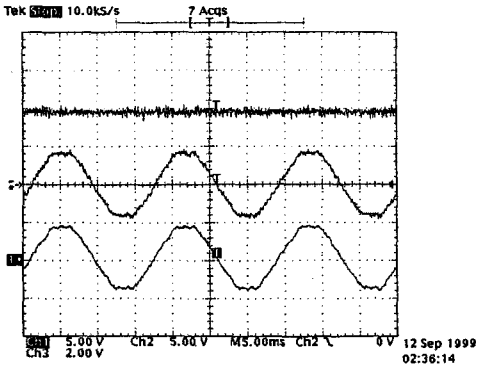

current : 7.5 [A/div.]

torque : 1 [Nm/div.]

(a) When the coeeing torque is considered

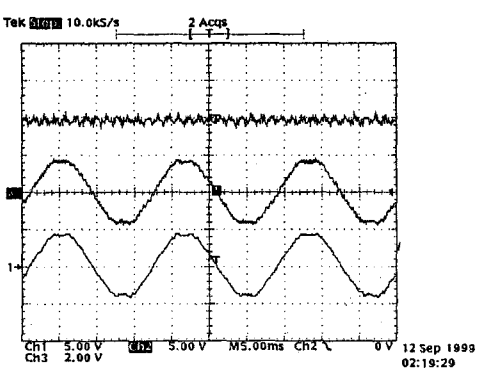

current : 7.5 [A/div.]

torque : 1 [Nm/div.]

(b) When the cogging torque is not considered

Fig. 10 The experimental results of the proposed control scheme of BLPM when the motor speed is 1800 rpm, the load torque is 2 Nm

controller and its interfaces are insulated against the electric shock and noise. The I/O controllers are implemented by using an erasable programmable logic device. The measured motor current, speed and rotor position are measured and transferred to the DSP controller from the insulated sensors via a 12 bit A/D converter (MAX 120 CNG) at every sampling period.

The experimental results are shown to validate the proposed method. Experiments are performed at the speed of 1,800 rpm and the load torque of 1 and 2 N. m. Figures 9(a) and (b) show the developed torque measured at the observer terminals together with the reference and motor current waveforms for when the cogging torque is considered and not considered, respectively. It is clear from the figures that the both motor currents are tracking the reference currents satisfactorily and they can deliver the load torque of 1 Nm. The torque ripple caused by the high frequency switching is included in both cases. In particular, the effect of the cogging torque on the torque ripple is clearly visible.

Figures 10(a) and (b) show the experimental

results when the load torque is increased to 2 Nm with the speed unchanged. It is also clear from the figures that both torque waveforms have the same tendency as in the former case and due to the increased load torque the ratio of the cogging torque to the load torque is relatively small.

These instantaneous torque profiles are calculated using measured phase currents and

back EMFs, mechanical speed and rotor position in the DSP. They are also measured from the DSP terminals. The obtained torque profiles are not a true shaft torque, because the torque components caused by the noise, mechanical damping and so on are not included. However, the effects of these torque components can be neglected. The torque profiles are in good agreement with those of Fig. 6(c) and only the ripple component due to the current deviation from the reference value is added to the average torque. However, its magnitude is also insignificant compared with the total torque and can be reduced by setting the current bandwidth to be confined to a small value.

5. Conclusions

In this paper, a novel optimal current excitation scheme of the BLPM for producing loss-minimized ripple-free torque based on the d-q-0 reference frame is presented. The optimized phase current waveforms that are obtained by the proposed method can aerve as reference values and the motor winding currents are forced to track it by the delta modulation technique. The proposed control scheme for the torque ripple elimination is shown to be simple and yet effective. The validity of the proposed control scheme is demonstrated by the simulation and experimental results.

Acknowledgments

This work was supported in part by the POSCO Chair Professor Research Fund of Pusan National University and ERC/Net Shape & Die Manufacturing, and in part by the Brain Korea 21 Project.

References

Bolton, H. R., and Ashen, R. A., 1984, "Influence of Motor Design and Feed-Current Waveform on Torque Ripple in Brushless DC Drive," *Proc. of IEE*, Vol. 131, Part B, No. 3, pp. 82~90.

Hanselman, D. C., 1994, "Minimum Torque Ripple, Maximum Efficiency Excitation of Brushless Permanent Magnet Motors," *IEEE Trans. Ind. Applicat.*, Vol. 41, No. 3, pp. 292~300.

Hanselman, D., Hung, J. Y., and Keshura, M., 1992, "Torque Ripple Analysis in Brushless Permanent Magnet Motor Drive," *Proc. ICEM* 92, Manchester, UK, pp. 823~827.

Hung, J. Y., and Ding, Z., 1992, "Minimization of Torque Ripple in Permanent Magnet Motors," *Proc. 18th IEEE Industrial Electronics Conf.*, San Diego, CA, pp. 459~463.

Jahns, T. M., 1984, "Torque Production in Permanent Magnet Synchronous Motor Drives with Rectangular Current Excitation," *IEEE Trans. Indust. Applicat.*, Vol. 20, No. 4, pp. 803~813.

Le-Huy, H., Perret, R., and Feuillet, R., 1986, "Minimization of Torque Ripple in Brushless DC Motor Drive," *IEEE Trans. Indust. Applicat.*, Vol. 22, No. 4, pp. 748~755.

Appendix

Parameters of BLPM

Rated output power	P_o	400 W
Rated voltage	V	100 V
Rated current	I	5 A
Resistance per phase	R	2.5 Ω
Inductance	L	13.8mH
Rated speed	N_r	1500r/min
Rated torque	T	2 Nm
Moment of inertia	J	0.0006Kgm^2